Re-excitation of localized electrons in SnO_2quantum dots for enhanced water photolysis activity

Xianqun Chen,[1,2] Liping Li,[1] Yuelan Zhang,[1] Yangsen Xu,[1] Guangshe Li*[1,3]

[1]*Key Laboratory of Design and Assembly of Functional Nanostructures, Fujian institute of Research on the Structure of Matter, Chinese Academy of Sciences, Fuzhou, 350002, P.R. China*

[2]*College of Materials Science and Engineering, Fujian Normal University, Fuzhou 350007, P. R. China*

[3]*State Key Laboratory of Inorganic Synthesis and Preparative Chemistry, College of Chemistry, Jilin University, Changchun 130012, P.R. China*

Supporting Information

1. XRD and TG analysis of SCTX

XRD patterns of SCTX are displayed in Figure S1.The presence of two sets of diffraction peaks that could beascribed to SnO_2 and g-C_3N_4, respectively, demonstrated the formation of hybrids between SnO_2 nanoparticles and g-C_3N_4.Furthermore, thermal gravities measurements (Figure S2) shows that the g-C_3N_4 becomes unstable when the heat temperature above 500℃.The mass of hybrids SCT3.0, SCT8.0 and SCT18.0decreased rapidly in the temperature range 500℃to 660℃， indicating that the combustion of g-C_3N_4occurred in this temperature range.[1]All samples exhibited a weight losses of about 60%, confirmed the 40% mass ratios of SnO_2 in the corresponding hybrids, which is consistent withinitial mass ratio of SnO_2.Based on the data analysis results in reference[2], the wide combustion temperature edge of SCT-18.0 should beattributed to the tight coupling between SnO_2 and g-C_3N_4.

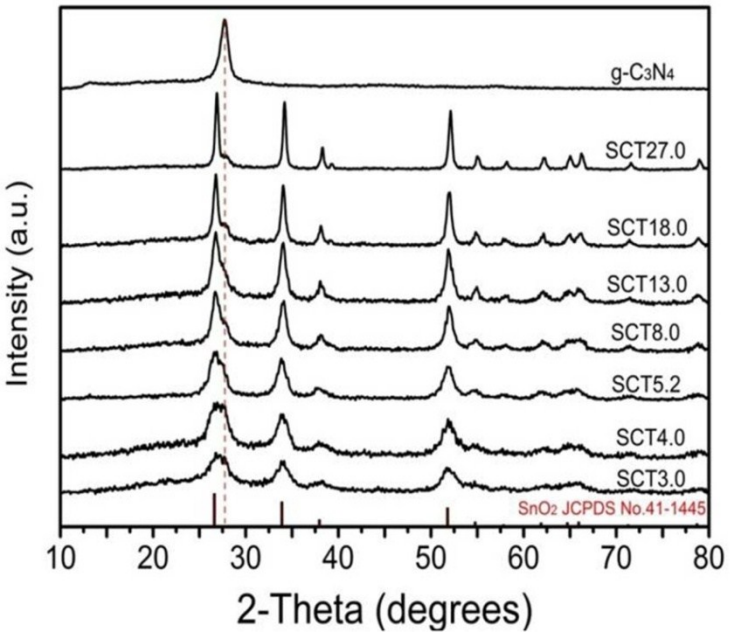

Figure S1. XRD patternsof SnO_2-X/g-C_3N_4 hybrids (SCTX).

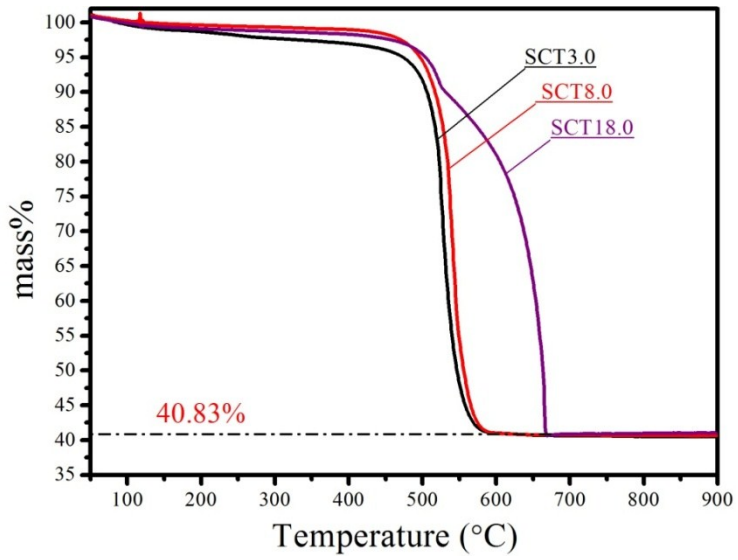

Figure S2. Thermal Gravity (TG) curves of SCT3.0, SCT8.0 and SCT18.0.

2 O1s XPS spectra

The signal at 531.5 eV presents the adsorbed oxygen species (OH^-) caused by oxygen vacancy,[3]

and its relative integrate areas of absorbed oxygen species to the lattice oxygen decrease from 45.6 to 19.3, which can reflect a decreased oxygen vacancy concentration caused by SnO_2 grain growth.

Table S1. Binding energy (B.E.), full width at half maximum (FWHM) and integral areas of O1s core levels for samples SCT3.0, SCT8.0, SCT13.0, SCT18.0.

Peak	Components	B.E. (eV)	FWHM (eV)	Area ratio (%)
O1s (SCT3.0)	$O\text{-}Sn^{4+}$	530.2	1.5	37.2
	OH^-	531.5	1.9	45.6
	H_2O	532.8	1.9	17.2
O1s (SCT8.0)	$O\text{-}Sn^{4+}$	530.2	1.7	45.8
	OH^-	531.4	1.8	41.7
	H_2O	532.7	2.0	12.5
O1s (SCT13.0)	$O\text{-}Sn^{4+}$	530.2	1.9	53.7
	OH^-	531.3	1.8	33.5
	H_2O	532.7	1.8	12.9
O1s (SCT18.0)	$O\text{-}Sn^{4+}$	530.2	2.0	71.5
	OH^-	531.5	1.7	19.3
	H_2O	532.7	1.9	9.2

3. Morphologies of the samples

The morphologies of hybrids SCT4.0, SCT13.0 and SCT18.0 were directly observed by TEM and HRTEM. As illustrated in Figure S3, SnO_2 particles (the black particles) in samples SCT4.0, SCT13.0 and SCT18.0 were successfully dispersed onto the stacked g-C_3N_4 layers (the gray color part, as indicated by the report of reference 4) even though some of SnO_2 nanoparticles were agglomerated.XRD analysis demonstrated that the crystallinityof SnO_2nanocrystals in hybrids was

enhanced with theircoarsening, which infersthat the surface defect concentration could were also reduced. Carefully examining the HRTEM image of Figure S4(c) for SCT4.0, it can be found that the atom spots in (110) plane are not continues, and a high density of dark holes (as marked by the white circles). These dark holes could be well-correlated to the oxygen vacancy sites. Using HRTEM analysis to demonstrate the existence of surface oxygen vacancy defects for nano-oxides has been reported in previous investigation.[5]Comparing toSCT4.0, the defect concentration in SCT13.0(Figure S4f)ismuch low. Alternatively, HRTEMof SCT18.0 in Figure 5(i)shows a nearly perfect atom arrangement in (110) lattice plane, suggesting the defect almost disappeared. These observations approved that annealing of SnO_2 in higher temperature could reduce the content of oxygen vacancy on the surface of SnO_2 nanocrystals.Figure S5 provides the grain size distribution of SnO_2nanocrystals in SCT4.0, SCT13.0 and SCT18.0. The mean grain size of SnO_2 in SCT4.0 is 3.9 nm, which issmaller than that of 12.6 nm in SCT13.0. The mean grain size of SnO_2 belong to SCT-18.0 is 20.5 nm, which is larger than that that calculated via XRD data broadening.

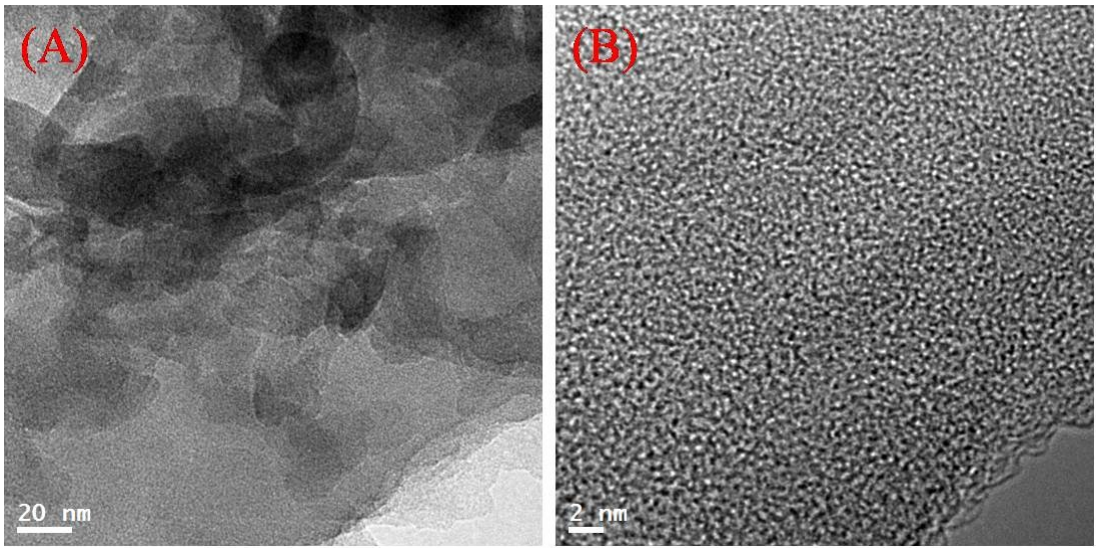

Figure S3.(A) TEM and (B) HRTEM image of g-C_3N_4.

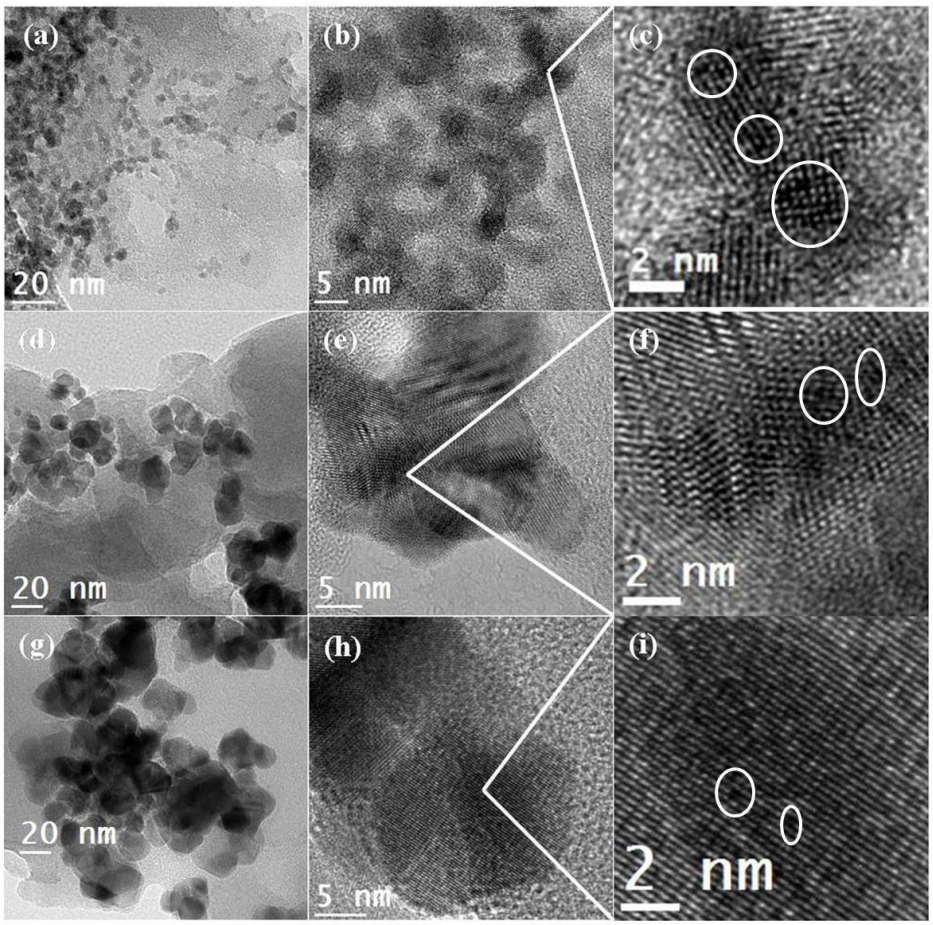

Figure S4.TEM, HRTEM and local magnified images for samples: (a, b, c) SCT4.0, (d, e, f) SCT13.0 and (g, h, i) SCT18.0.

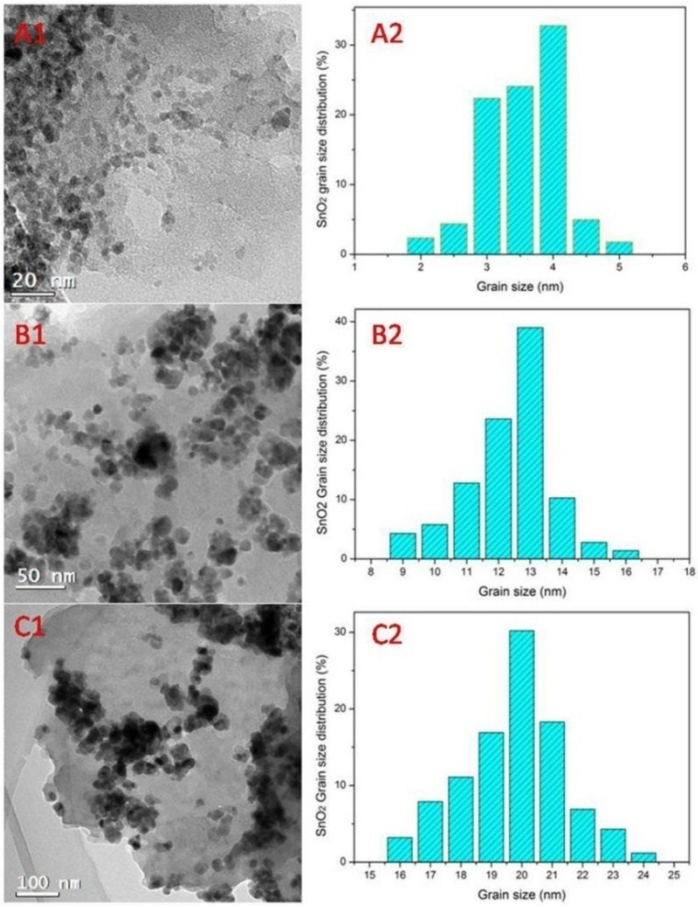

Figure S5. The grain size distribution of SnO_2-4.0 (A1,A2), SnO_2-13.0 (B1,B2) and SnO_2-18.0 (C1, C2) when supported on g-C_3N_4.

Table S2. The BET specific area measured for samples SCT-4.0, SCT-13.0 and SCT-18.0.

Sample	SCT4.0	SCT-13.0	SCT-8.0
BET specific area (m^2/g)	105	72	45

4 Photocatalytic activity of SnO_2-8.0

The activity of as-prepared SnO_2-8.0 in hydrogen generation from water splitting is really poor to yield hydrogen of 3.0μmol and 0 μmol after irradiation for 5h under the 260 nm and 420 nm light, which approved its appropriate energy band position for hydrogen generating from water photolysis.

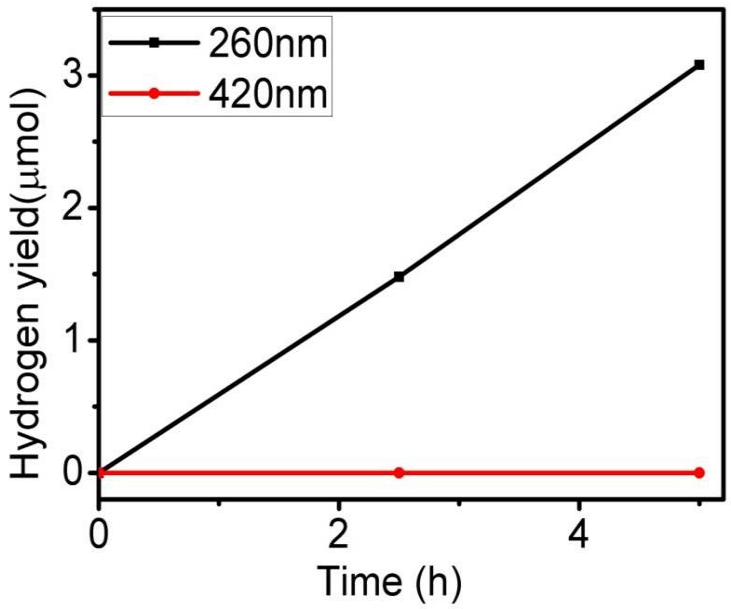

Figure S6. Catalytic hydrogen yield from water splitting for 100mg of as-prepared SnO_2 under ultraviolet (λ>260 nm, the black line) and visible (λ>420 nm, the red line) light irradiation with 300W Xe lamp.

References

1. J. X. Sun, Y.P. Yuan, L.G. Qiu, X. Jiang, A.J. Xie, Y.H. Shen and J.F. Zhu, *Dalton. T*, 2012, 41, 6756-6763.

2.Y. He, L. Zhang, M. Fan,X.Wang, M. L. Walbridge, Q. Nong,Y. Wu, L. Zhao, *Sol. Energ. Mat.and Sol. C*, 2015, 137, 175-184.

3.Das, A; Bonu, V; Prasad, A. K; Panda, D; Dhara, S; Tyagi, A. K, *J. Mater. Chem. C*, 2014, 2(1), 164-171.

4.X. Wang, K. Maeda, X. Chen, K. Takanabe, K. Domen, Y. Hou, X. Fu and M. Antonietti, *J. Am. Chem.Soc*, *2009*, 131(5), 1680-1681.

5.N. J. Lawrence, J. R. Brewer, L. Wang, T.S. Wu, J. Wells-Kingsbury, M. M. Ihrig, G. Wang, Y. L. Soo, W.N. Mei and C. L. *Cheung, Nano. Lett*, 2011, 11(7), 2666-2671.